RESEARCH ARTICLE | *Integrative Cardiovascular Physiology and Pathophysiology*

VEGF nanoparticles repair the heart after myocardial infarction

Yasin Oduk,[1]* Wuqiang Zhu,[1]* Ramaswamy Kannappan,[1] Meng Zhao,[1] Anton V. Borovjagin,[1]
Suzanne Oparil,[2] and Jianyi (Jay) Zhang[1]

[1]*Department of Biomedical Engineering, School of Medicine and School of Engineering, University of Alabama at Birmingham, Birmingham, Alabama; and* [2]*Vascular Biology and Hypertension Program, Division of Cardiovascular Disease, Department of Medicine, University of Alabama at Birmingham, Birmingham, Alabama*

Oduk Y, Zhu W, Kannappan R, Zhao M, Borovjagin AV, Oparil S, Zhang J. VEGF nanoparticles repair the heart after myocardial infarction. *Am J Physiol Heart Circ Physiol* 314: H278–H284, 2018. First published November 3, 2017; doi:10.1152/ajpheart.00471.2017.— Vascular endothelial growth factor (VEGF) is a well-characterized proangiogenic cytokine that has been shown to promote neovascularization in hearts of patients with ischemic heart disease but can also lead to adverse effects depending on the dose and mode of delivery. We investigated whether prolonged exposure to a low dose of VEGF could be achieved by encapsulating VEGF in polylactic coglycolic acid nanoparticles and whether treatment with VEGF-containing nanoparticles improved cardiac function and protected against left ventricular remodeling in the hearts of mice with experimentally induced myocardial infarction. Polylactic coglycolic acid nanoparticles with a mean diameter of ~113 nm were generated via double emulsion and loaded with VEGF; the encapsulation efficiency was $53.5 \pm 1.7\%$ (107.1 ± 3.3 ng VEGF/mg nanoparticles). In culture, VEGF nanoparticles released VEGF continuously for at least 31 days, and in a murine myocardial infarction model, VEGF nanoparticle administration was associated with significantly greater vascular density in the peri-infarct region, reductions in infarct size, and improvements in left ventricular contractile function 4 wk after treatment. Thus, our study provides proof of principle that nanoparticle-mediated delivery increases the angiogenic and therapeutic potency of VEGF for the treatment of ischemic heart disease.

NEW & NOTEWORTHY Vascular endothelial growth factor (VEGF) is a well-characterized proangiogenic cytokine but has a short half-life and a rapid clearance rate. When encapsulated in nanoparticles, VEGF was released for 31 days and improved left ventricular function in infarcted mouse hearts. These observations indicate that our new platform increases the therapeutic potency of VEGF.

cardiac tissue; myocardial infarction; nanoparticle; revascularization; sustained release; vascular endothelial growth factor

INTRODUCTION

Whether the goal of regenerative myocardial therapy is to invigorate hibernating myocardium by restoring perfusion to the ischemic region or to replace the damaged muscle with transplanted cells or engineered tissue, the effectiveness of the treatment is crucially dependent on vascular growth. Vascular endothelial growth factor (VEGF) is among the most powerful and well-characterized proangiogenic cytokines (14, 15, 19) and has been associated with improvements in cardiac vascu-larization, but it can also lead to severe side effects, such as hypotension, limb edema, and retinopathy, or to the growth and metastasis of malignant tumors (2, 7, 8, 10, 13, 25). VEGF overexpression has also been linked to a number of human diseases, including atherosclerosis, age-related macular degeneration, rheumatoid arthritis, and diabetic retinopathy (14), whereas both VEGF overexpression and deficiency in the glomeruli lead to renal disease in mice (6). Thus, the therapeutic use of VEGF requires precise dosing to ensure that patients receive the maximum possible benefit while avoiding safety concerns (4).

Evidence suggests that patients respond better to VEGF therapy when the treatment is administered via repeated infusions (10) or in a slow-release formulation (18) rather than as a single bolus dose. Longer exposure times may also yield benefits at lower plasma levels, which could reduce the risks associated with VEGF overdosing. The short half-life (33.7 ± 13.7 min in plasma) and rapid clearance rate (0.0206 min^{-1}) (5) of VEGF suggest that extended VEGF delivery will require a method for protecting the protein from the surrounding microenvironment. For the study presented here, we hypothesized that encapsulating VEGF in polylactic coglycolic acid (PLGA) nanoparticles would preserve its integrity and activity in vivo, thereby prolonging tissue exposure to the cytokine (Fig. 1). We also tested whether VEGF-containing nanoparticles can improve left ventricular (LV) function, limit adverse cardiac remodeling, and increase angiogenesis in mice with surgically induced myocardial infarction (MI).

METHODS

All procedures involving animals were approved by the Animal Resources Program of the University of Alabama at Birmingham and were consistent with the National Institutes of Health *Guide for the Care and Use of Laboratory Animals*. Because the experimental treatment consisted of the human variant of VEGF (hVEGF) and PLGA nanoparticles, in vivo experiments were performed with immunocompromised NOD/SCID mice (~25 g, up to 16 wk of age, The Jackson Laboratory, Bar Harbor, ME) to minimize the immune response. Human umbilical vein primary endothelial cells (HUVECs; PCS-100-010) were purchased from the American Type Culture Collection. PLGA (lactide-to-glycolide molar ratio: 50:50, molecular weight: 7,000–17,000) and polyvinyl alcohol (PVA; molecular weight: 89,000–98,000) were purchased from Fisher Scientific. hVEGF165 recombinant protein (19.2 kDa) and the human VEGF Quantikine ELISA Kit were purchased from R&D Systems. Vascular cell basal medium and the endothelial cell growth kit were purchased from Fisher Scientific. Coumarin-6 (molecular weight: 350.43) and
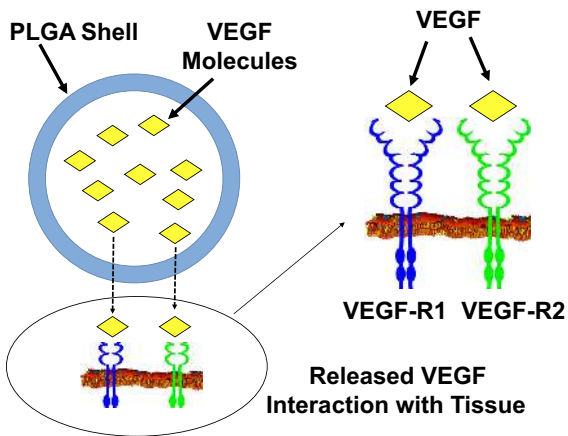
Fig. 1. The duration of vascular endothelial growth factor (VEGF) exposure is extended via encapsulation in polylactic coglycolic acid (PLGA) nanoparticles. VEGF-containing PLGA nanoparticles were prepared via a double emulsion (water/oil/water phase) technique. After administration, the encapsulated VEGF was protected from degradation and slowly released from the nanoparticles via diffusion through the polymer matrix, desorption of the adsorbed VEGF from the surface, degradation or erosion of the nanoparticle matrix, and the combination of erosion and diffusion, which prolonged the length of time that it was capable of interacting with VEGF receptors (VEGF-Rs) on the surface of cells at the site of administration.

dichloromethane were purchased from Sigma-Aldrich (St. Louis, MO). All other chemicals were obtained from commercial sources.

Preparation and Characterization of PLGA Nanoparticles

PLGA nanoparticles were prepared via a double emulsion (water/oil/water phase) technique. Briefly, a solution of PLGA (100 mg) in dichloromethane (5 ml) with or without VEGF (200 µl at 100 µg/ml) and with or without coumarin-6 (1 mg) was ultrasonicated at 40% amplitude in 40-s intervals with 20-s pauses for a total of 2 min; 20 ml of a 4% (wt/vol) PVA-water solution was then added, and the mixture was ultrasonicated on ice at 40% amplitude in ~40-s intervals with 20-s pauses for a total of 2 min. The mixture was transferred to 10 ml of a 4% (wt/vol) PVA-water solution and 30 ml of Milli-Q water to a 100-ml glass beaker and stirred for 4 h until the dichloromethane evaporated. The solution was then centrifuged at 1,000 g for 10 min to remove any aggregates, and the supernatant was removed and centrifuged at 45,000 g for 20 min to collect the nanoparticles. The nanoparticles were washed three times (to remove any PVA) by resuspending them in 50 ml of Milli-Q water and recollecting them via centrifugation at 45,000 g for 20 min and then frozen at $-80°C$ overnight, lyophilized for 48 h, and stored in Eppendorf tubes at $-80°C$.

Nanoparticle size measurements were performed via nanoparticle tracking analysis with a NanoSight NS300 Instrument (NanoSight, Wiltshire, UK); ζ potentials were determined with a Zetasizer Nano ZS (Malvern, Southborough, MA), and scanning electron microscopy was performed with a Quanta FEG 650 (FEI, Hillsboro, OR). The VEGF release profile was determined by suspending the VEGF nanoparticles in the release medium (deionized PBS with 0.1% BSA and 0.02% sodium azide), incubating them at 37°C with constant shaking, withdrawing, and replacing 900 µl of the medium at the indicated time points and then measuring VEGF levels in the withdrawn medium with a human VEGF ELISA kit.

In Vitro Analyses

Cell proliferation. HUVECs were seeded in 96-well (3×10^3 cells/well) or 8-well (2×10^5 cells/well) plates and cultured for 48 h with 30 ng/ml free VEGF protein, 1 mg/ml VEGF-loaded nanoparticles, which [based on the release profile determined in PBS (Fig. 2D)] would release 30 ng/ml VEGF during the culture period, or in the absence of VEGF (untreated). Proliferation was evaluated by counting the cells that stained positively for expression of the proliferation marker Ki67 and by measuring NADPH-dependent dehydrogenase activity. Ki67 expression was identified via immunofluorescence with anti-Ki67 primary antibodies (rabbit, IgG, ab16667, Abcam, Cambridge, MA) and FITC-conjugated secondary antibodies (donkey anti-rabbit, IgG, no. 711095152, Jackson ImmunoResearch, West Grove, PA). Dehydrogenase activity was measured with a MTS assay kit (G1112, Promega, Madison, WI).

Tube formation. HUVECs (1×10^5 cells/well) were seeded in 24-well plates that had been precoated with Matrigel and cultured for 16 h with 30 ng/ml free VEGF protein, 1 mg/ml VEGF-loaded nanoparticles, or in the absence of VEGF (untreated). Cells were stained with calcein AM dye, and tube formation was evaluated via fluorescence microscopy and bright-field microscopy with an Olympus IX83 microscope.

Nanoparticle uptake. HUVECs were seeded in 96-well plates (3×10^3 cells/well), allowed to grow until confluent, and then cultured at 37°C with 2 or 20 µg/ml nanoparticles that had been loaded with coumarin-6 or with both coumarin-6 and VEGF. After the 6-h culture period, cells were washed twice with PBS and solubilized with 5% SDS in 0.1 M NaOH. Nanoparticle uptake was quantified by analyzing the fluorescence intensity of the cell lysates. Measurements were normalized to the fluorescence intensity of an equivalent amount of coumarin-6-loaded nanoparticles and expressed as a percentage.

Mouse MI Model and Analyses

Mice were anesthetized with inhaled isoflurane (2%), intubated, ventilated, and placed in a right lateral decubitus position on a heating pad. A left thoracotomy was performed, and the left anterior descending coronary artery was ligated as previously described (21). Animals were treated with one of three doses of VEGF nanoparticles (0.6, 2.4, or 6 ng) or allowed to recover without any experimental treatment. The nanoparticles were injected into the peri-infarct region with a modified Hamilton needle; the pectoral muscles and skin were closed, and a combination of carprofen and buprenorphine was provided for pain control. The fifth group of animals ($n = 6$) underwent all surgical procedures necessary for MI induction except for the ligation step.

Echocardiography. Echocardiography was performed before and 4 wk after surgery to assess LV function. Animals were lightly anesthetized with 0.5–1% inhaled isoflurane, and heart rates were stabilized at 400–500 beats/min. B-mode and two-dimensional M-mode images were obtained from the parasternal long-axis and short-axis views at the midpapillary level of the LV and analyzed with a Vevo 2100 system (Visualsonics, Toronto, ON, Canada). Measurements were performed offline with Vevo 770 (version 3.0.0) quantification software and used to calculate LV ejection fraction (LVEF), LV fractional shortening (LVFS), LV end-diastolic diameter (LVEDD), and LV end-systolic diameter (LVESD), as previously described (23).

Infarct size and wall thickness. Immediately after the second echocardiographic procedure, hearts were harvested, frozen in 30% sucrose, embedded, and cut into 10-µm sections; six sections from the apex to the base of the heart were stained with Sirius red and fast green. The area of the infarct (i.e., the region stained with Sirius red) was quantified as previously described (12), normalized to the area of the LV, and expressed as a percentage. Wall thickness was measured in fast green Sirius red-stained sections by taking the average length of five segments along evenly spaced radii from the center of the LV through the infarcted LV free wall (22). Analyses were performed with National Institutes of Health Image (24) and ImageJ software.

Vascular density. Six sections from each heart were stained with fluorescent anti-CD31 antibodies; vascular density was then expressed as the number of CD31-positive vascular structures per unit area in the border zone of infarction (20, 21).
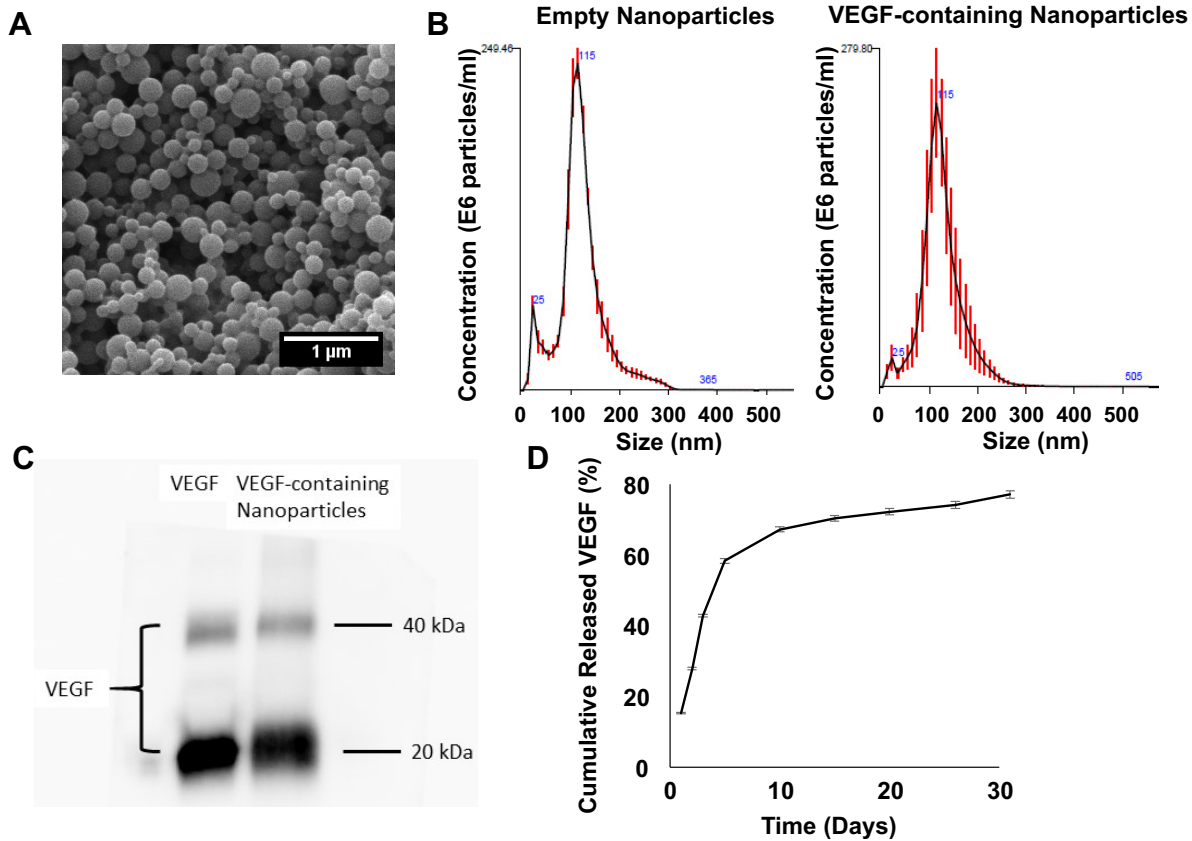
Fig. 2. Polylactic coglycolic acid (PLGA) nanoparticles release measurable amounts of vascular endothelial growth factor (VEGF) for up to 31 days in vitro. The size distribution (*A*) of the PLGA nanoparticles was evaluated via nanoparticle tracking analysis (*B*). *C*: the amount of VEGF encapsulated by the nanoparticles (*right* lane) was compared with the amount present in the solution before the encapsulation procedure (*left* lane) via Western blot. The two bands correspond to fully dissociated monomers (20 kDa) and undissociated dimers (40 kDa) of human VEGF. *D*: VEGF-containing nanoparticles were incubated at 37°C in culture medium for 31 days. The cumulative amount of VEGF released from the VEGF nanoparticles was determined via ELISA assessments of aliquots taken from the release medium at the indicated time points and presented as a percentage of the total amount of VEGF present in the nanoparticles at the beginning of the release experiment.

Statistical Analysis

Data are presented as means $\pm$ SE. Comparisons between groups were evaluated via one-way ANOVA with the Bonferroni correction. Calculations were performed with GraphPad Prism 7 software. *P* values of <0.05 were considered significant.

RESULTS

Nanoparticle-Encapsulated VEGF Is Slowly Released for at Least 31 Days

PLGA nanoparticles (Fig. 2*A*) with mean diameters of 115.6 $\pm$ 1.3 and 113.1 $\pm$ 5.2 nm (Fig. 2*B* and Table 1) were generated by a double emulsion technique; the encapsulation efficiency (i.e., the amount encapsulated/total amount available $\times$ 100%) was 53.5 $\pm$ 1.7% (Fig. 2*C* and Table 1), and the concentration of encapsulated VEGF was 107.1 $\pm$ 3.3 ng protein/mg nanoparticles (Table 1). When 1 mg of VEGF-loaded nanopar-

ticles was incubated in 1 ml PBS at 37°C, 42.9% of the encapsulated VEGF was released during the first 3 days and 67.3% was released by *day 10* (Fig. 2*D*), which corresponded to release rates of 13.5–16.4 $ng \cdot ml^{-1} \cdot day^{-1}$ from *day 0* to *day 3* and 1.9–8.3 $ng \cdot ml^{-1} \cdot day^{-1}$ from *day 3* to *day 10* (Table 2). The rate of VEGF release at later time points ranged from 0.4 to 0.7 $ng \cdot ml^{-1} \cdot day^{-1}$ through *day 31*.

Nanoparticle-Encapsulated VEGF Is More Potent Than the Free Protein for Promoting Proangiogenic Activity in Cultured HUVECs

The effects of nanoparticle-mediated VEGF delivery on endothelial cell proliferation and tube formation were evaluated in vitro by culturing HUVECs for 48 h with 30 ng/ml free VEGF protein, 1 mg/ml VEGF-loaded nanoparticles, which [based on the release profile determined in PBS (Fig. 2*D*)] would release 30 ng/ml VEGF during the culture period, or in

Table 1. *Polylactic coglycolic acid nanoparticles: physical characteristics*

Nanoparticle Contents	Size, nm	Encapsulation Efficiency, %*	VEGF Concentration, ng/mg	Surface Charge, mV
Empty	115.6 $\pm$ 1.3	NA	NA	−56.2 $\pm$ 8.5
VEGF	113.1 $\pm$ 5.2	53.5 $\pm$ 1.7	107.1 $\pm$ 3.3	−55.4 $\pm$ 8.2

VEGF, vascular endothelial growth factor. *Encapsulation efficiency = (VEGF encapsulated in nanoparticles/VEGF fed) $\times$ 100.

Table 2. *VEGF release from polylactic coglycolic acid nanoparticles*

Time Period, days	VEGF Released	
	ng/ml	%
0–1	16.38 ± 0.31	15.29 ± 0.42
1–2	13.49 ± 0.48	12.59 ± 0.45
2–3	16.06 ± 0.24	14.99 ± 0.23
3–5	16.58 ± 0.64	15.48 ± 0.60
5–10	9.55 ± 0.32	8.91 ± 0.30
10–15	3.26 ± 0.22	3.05 ± 0.21
15–20	2.02 ± 0.15	1.89 ± 0.14
20–26	2.05 ± 0.33	1.91 ± 0.31
26–31	3.20 ± 0.16	2.99 ± 0.15

VEGF, vascular endothelial growth factor.

the absence of VEGF (untreated). Proliferation was significantly greater in VEGF nanoparticle-treated cells than when cells were cultured with the VEGF protein or in the absence of VEGF (untreated) (Fig. 3, *A* and *B*), whereas tube formation after treatment with VEGF nanoparticles or free VEGF was similar and significantly greater than in untreated cells (Fig. 3*C*). Furthermore, experiments with nanoparticles containing the fluorescent marker coumarin-6 with or without VEGF indicated that the mechanism by which the contents of the nanoparticles are taken up by the cells is saturable: up to 84% of the fluorescence signal was internalized when cells were cultured with 2 μg/ml nanoparticles compared with 12% when the nanoparticle concentration was 20 μg/ml (Fig. 3*D*).

VEGF Nanoparticles Improve Recovery From MI in Mice

To determine whether nanoparticle-mediated VEGF delivery can improve recovery from ischemic myocardial injury, MI was surgically induced in the hearts of mice by ligating the left anterior descending coronary artery; animals were then treated with one of three doses of VEGF nanoparticles [MI + low-dose VEGF nanoparticles (0.6 ng): $n = 9$, MI + medium-dose VEGF nanoparticles (2.4 ng): $n = 9$, or MI + high-dose VEGF nanoparticles (6 ng): $n = 8$] or allowed to recover without VEGF nanoparticle administration (MI: $n = 13$). Three animals (MI: $n = 2$ and MI + low-dose VEGF nanoparticles: $n = 1$) died within 3 days of MI induction, and six more animals (MI: $n = 2$, MI + low-dose VEGF nanoparticles: $n = 1$, and MI + high-dose VEGF nanoparticles: $n = 3$) died within 2 wk of MI induction (Fig. 4). At *week 4*, echocardiographic assessments of LVEF, LVFS, LVEDD, and LVESD were significantly greater in each of the three VEGF nanoparticle treatment groups than in the untreated group (Fig5*A*). Furthermore, the nanoparticle-encapsulated VEGF could be identified at the site of administration (Fig. 6), and all three VEGF nanoparticle doses were associated with significantly smaller infarct sizes and significantly greater wall thicknesses (Fig. 5*B*), significantly greater measurements of vascular density in the region bordering the infarct (Fig. 5*C*), and significantly lower heart weight-to-body weight ratios (Fig. 5*D*). However, the benefits associated with VEGF nanoparticle treatment were not dose dependent: LVEF, LVFS, LVESD, LVEDD, infarct size, wall thickness, and heart weight-to-body weight ratios in the three
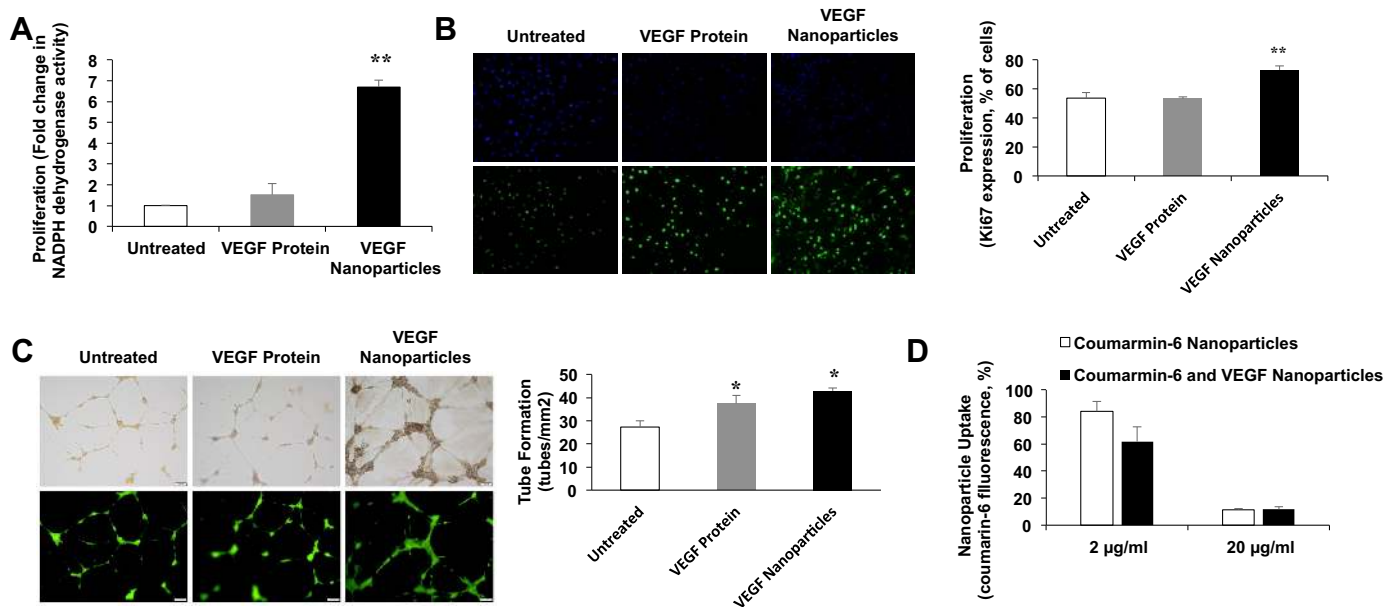

Fig. 3. Vascular endothelial growth factor (VEGF) nanoparticles are more potent than free VEGF protein for stimulating the proangiogenic activity of cultured human umbilical vein primary endothelial cells (HUVECs). *A* and *B*: HUVECs were cultured for 48 h with 30 ng/ml free VEGF protein, 1 mg/ml VEGF-loaded nanoparticles (VEGF nanoparticles), which (based on the release profile determined in PBS) would release 30 ng/ml VEGF during the culture period, or in the absence of VEGF (untreated). Proliferation was evaluated by measuring the level of NADPH-dependent dehydrogenase activity (*A*) and immunofluorescent analysis of Ki67 expression (*B*). Dehydrogenase measurements are expressed as fold changes from measurements in untreated cells. *C*: HUVECs were cultured on Matrigel in 24-well plates with VEGF protein, VEGF nanoparticles, or in the absence of either treatment for 16 h and stained with fluorescent dye (calcein AM). Tube formation was then quantified. *D*: HUVECs were seeded in 96-well plates, allowed to grow until confluent, and cultured at 37°C with 2 or 20 μg/ml nanoparticles loaded with either coumarin-6 or both coumarin-6 and VEGF. Cells were then lysed, and nanoparticle uptake was determined by measuring the intensity of coumarin-6 fluorescence. Measurements were normalized to the fluorescence intensity of an equivalent amount of coumarin-6-loaded nanoparticles and expressed as a percentage. *$P < 0.05$ vs. untreated; **$P < 0.05$ vs. untreated and free VEGF protein. Each experiment was performed in triplicate.
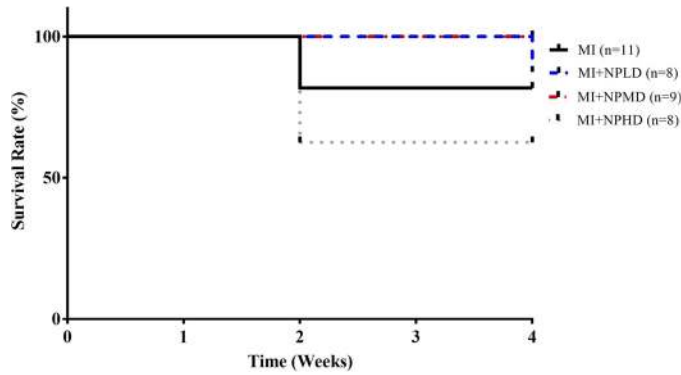
Fig. 4. Kaplan-Meyer survival curves. Myocrdial infarction (MI) was surgically induced in the hearts of mice by ligating the left anterior descending coronary artery; animals were then treated with one of three doses of vascular endothelial growth factor (VEGF) nanoparticles [MI + low-dose VEGF nanoparticles (NPLD; 0.6 ng), MI + medium-dose VEGF nanoparticles (NPMD; 2.4 ng), or MI + high-dose VEGF nanoparticles (NPHD; 6 ng)] or allowed to recover with no experimental treatment (MI). The number of animals in each group that continued to survive was recorded at weekly time points until animals were euthanized at *week 4*.

dose groups were similar, vascular density was significantly greater in animals treated with the lowest dose of VEGF nanoparticles than in the medium- and high-dose groups, and heart weight-to-body weight ratios in low-dose animals did not differ significantly from the ratios in sham-operated animals.

DISCUSSION

Because of their porosity, hydrogels have been widely investigated for use as a drug delivery vehicle and could provide an additional level of flexibility and refinement for prolonging the duration of exposure to biological molecules, which are typically less stable than pharmacological agents (3). Furthermore, nanoparticle-based systems that promote the revascularization of ischemic myocardium after MI by enabling the sustained local release of a therapeutic cytokine would be an attractive and novel approach to infarcted cardiac tissue regeneration (11). In the present study, we establish the proof of concept of a new, nanoparticle-based therapeutic platform for localized delivery of the proangiogenic cytokine VEGF to in-
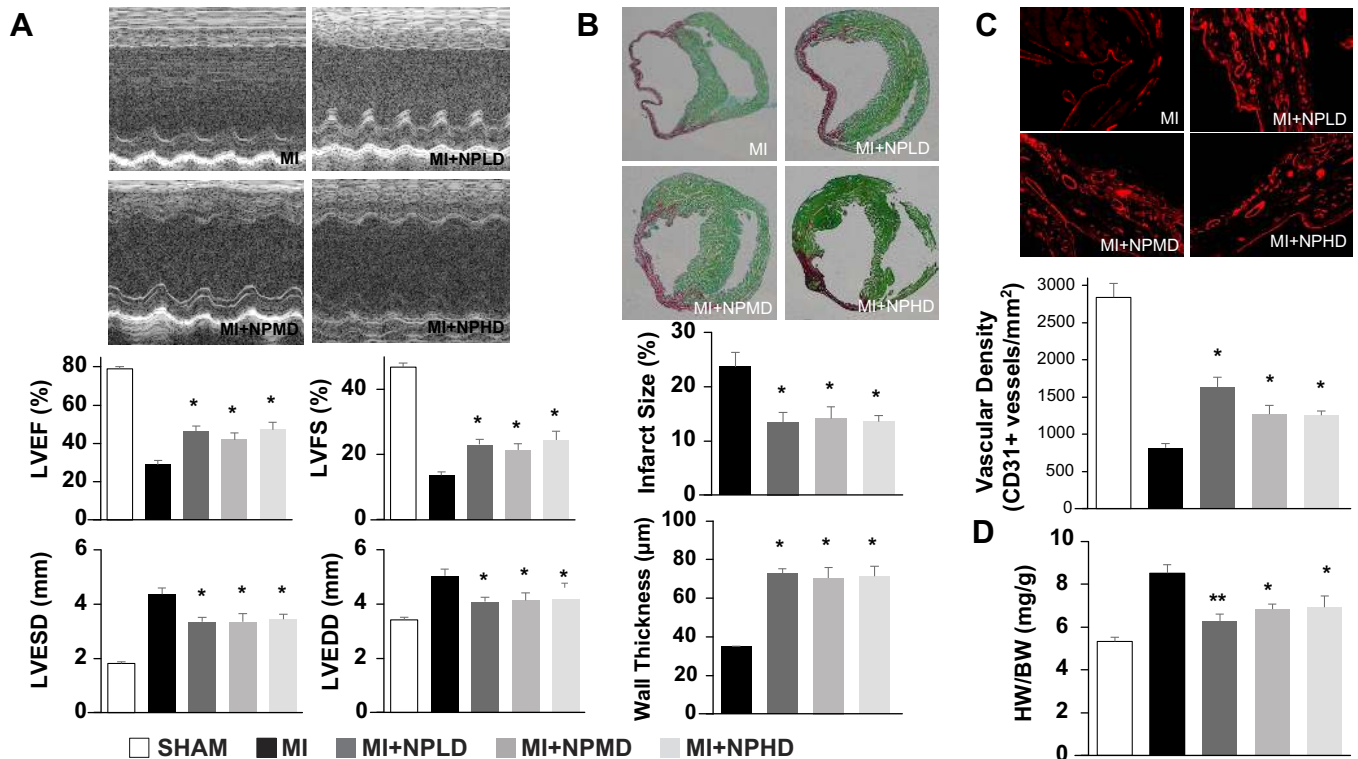

Fig. 5. Vascular endothelial growth factor (VEGF) nanoparticles improve recovery from myocardial infarction (MI) in mice. MI was surgically induced in the hearts of mice by ligating the left anterior descending coronary artery; animals were then treated with one of three doses of VEGF nanoparticles [MI + low-dose VEGF nanoparticles (NPLD; 0.6 ng), MI + medium-dose VEGF nanoparticles (NPMD; 2.4 ng), or MI + high-dose VEGF nanoparticles (NPHD; 6 ng)] or allowed to recover with no experimental treatment (MI). The fifth group of animals (sham) underwent sham surgery. *A*: left ventricular (LV) ejection fraction (LVEF), LV fractional shortening (LVFS), LV end-diastolic diameter (LVEDD), and LV end-systolic diameter (LVESD) were evaluated 4 wk after MI via echocardiography (*$P < 0.05$ vs. MI and sham). *B–D*: mice were euthanized 4 wk after MI. *B*: infarct size was evaluated in Sirius red- and fast green-stained sections and presented as a percentage of the total LV surface area. Wall thickness was measured in fast green Sirius red-stained sections by taking the average length of five segments along evenly spaced radii from the center of the LV through the infarcted LV free wall (*$P < 0.05$ vs. MI). *C*: vascular density was evaluated in sections from the border zone of ischemia that had been stained for expression of the endothelial marker CD31 (*$P < 0.05$ vs. MI). *D*: myocardial hypertrophy was evaluated as the ratio of the whole heart weight to body weight (HW/BW) (*$P < 0.05$ vs. MI and sham; **$P < 0.05$ vs. MI but not vs. sham).
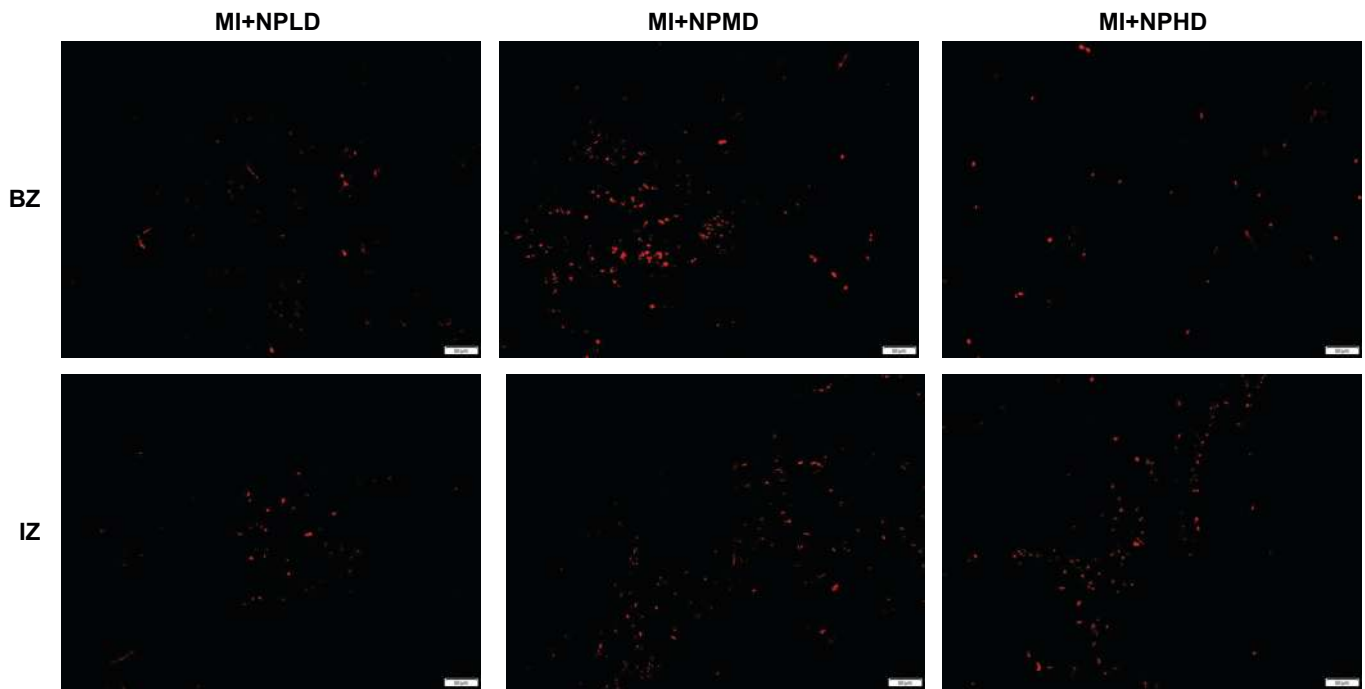
Fig. 6. Nanoparticle-encapsulated vascular endothelial growth factor (VEGF) was detectable 4 wk after administration to infarcted mouse hearts. Because the nanoparticles were loaded with the human variant of VEGF, the administered protein was detected in sections from the border zone (BZ) and infarcted zone (IZ) of hearts from animals in the low-dose (NPLD), medium-dose (NPMD), and high-dose (NPHD) groups at *week 4* after nanoparticle administration via staining with human-specific anti-VEGF antibodies (red). Bar, 50 μm.

farcted heart tissue. Future studies will determine the feasibility of combining our VEGF nanoparticle system with proangiogenic microRNAs for the treatment of ischemic heart disease.

The development of a dependable system for prolonged local delivery of therapeutic proteins such as VEGF in injured hearts has been a goal for several research groups in the field of cardiovascular therapy. Recent studies have shown that both intramyocardial injections (17) and patch-mediated transplantation (16) of VEGF-containing microparticles (~3–5 μm in diameter) led to improvements in cardiac function and other benefits when tested in rat models of MI. In both cases, estimates of the protein release rate suggested that ~50% of the microparticle-encapsulated protein was released in the first 4–26 h and that the duration of VEGF exposure was limited to 5–10 days. In contrast, we showed that when VEGF was encapsulated in PLGA nanoparticles, only 15% of the protein was released on *day 1*; <50% was released through *day 3*, and ~0.6 ng·ml^{-1}·day^{-1} continued to be released from *day 26* to *day 31*. Thus, on the basis of the volume of the injections (15 μl), the concentration of VEGF (4 mg/ml), and the VEGF release profile observed when the nanoparticles were cultured in PBS, we calculated that infarcted regions in the hearts of the high-dose nanoparticle-treated mice were exposed to ~100–200 pg of VEGF after *day 26*. Although we acknowledge that the release profile observed in PBS may be altered by properties of the microenvironment in infarcted tissues and cell culture medium, such as pH and cellular uptake, this sustained, low-level release of VEGF may play a significant role in its therapeutic effects. Nanoparticles have a much larger cumulative surface area than an equivalent volume of microparticles, which may increase both the total amount of VEGF that they can carry and their ability to interact with the surrounding tissue.

Our experiments with cultured HUVECs demonstrated that nanoparticle encapsulation increased the biological activity of VEGF; both proliferation and tube formation were significantly higher when cells were treated with VEGF-containing nanoparticles than when an equivalent amount of free VEGF peptide was added to the medium, perhaps because the nanoparticles protected the VEGF from degradation. Furthermore, although the delivery of nanoparticle-encapsulated VEGF to cells occurs via diffusion through the polymer matrix, desorption of the adsorbed VEGF from the surface, degradation or erosion of the nanoparticle matrix, and the combination of erosion and diffusion (1), we found evidence of nanoparticle uptake by HUVECs, which could effectively increase the VEGF concentration at the site of administration by preventing the nanoparticles from being cleared into the circulation. The encapsulated VEGF may also bind to VEGF receptors during cellular uptake or after release into the cell interior and travel to the cell membrane before binding to VEGF receptors both inside and outside the cell.

Our in vitro observations were consistent with the results from our rodent MI model, in which VEGF nanoparticle administration was associated with significant improvements in cardiac performance, angiogenesis, infarct size, wall thickness, and cardiac hypertrophy (heart weight-to-body weight ratios), regardless of the dose. Notably, measurements of cardiac function (LVEF, LVFS, LVESD, and LVEDD) were similar in all three VEGF nanoparticle dosing groups, whereas the effect on vascular density was greatest in animals that received the lowest dose; heart weight-to-body weight ratios in the lowest dose group did not differ significantly from the ratios in sham-operated animals. Although the mechanisms responsible for this apparently biphasic relationship between VEGF nanoparticle dose and vessel density remain unclear, these results are consistent with a previous report (9) indicating that the therapeutic benefits of VEGF administration decline at

higher doses. Our observations also suggest that the therapeutic effect of VEGF nanoparticle delivery may have been saturated at the two higher doses and that the duration of VEGF exposure may be at least as important as the amount of VEGF administered.

In conclusion, collectively, the experiments described in this report comprise a proof-of-concept study for a new therapeutic platform, PLGA nanoparticles, that can be used for the local delivery of biologically active proteins and peptides. Our results suggest that nanoparticle-mediated delivery increases the angiogenic and therapeutic potency of VEGF, which may enhance the benefits and limit the risks of VEGF therapy by reducing the dose administered to patients. Additional preclinical and clinical investigations of this promising new delivery system are warranted.

DISCLOSURES

No conflicts of interest, financial or otherwise, are declared by the authors.

AUTHOR CONTRIBUTIONS

Y.O., W.Z., R.K., and J.Z. conceived and designed research; Y.O., W.Z., and M.Z. performed experiments; Y.O. and W.Z. analyzed data; Y.O., W.Z., R.K., M.Z., A.V.B., S.O., and J.Z. interpreted results of experiments; Y.O. prepared figures; Y.O. drafted manuscript; Y.O., W.Z., R.K., A.V.B., S.O., and J.Z. edited and revised manuscript; J.Z. approved final version of manuscript.

REFERENCES

1. **Asmatulu R, Fakhari A, Wamocha HL, Chu HY, Chen YY, Eltabey MM, Hamdeh HH, Ho JC.** Drug-carrying magnetic nanocomposite particles for potential drug delivery systems. *J Nanotechnol* 2009: 1–6, 2009. doi:10.1155/2009/238536.
2. **Baumgartner I, Rauh G, Pieczek A, Wuensch D, Magner M, Kearney M, Schainfeld R, Isner JM.** Lower-extremity edema associated with gene transfer of naked DNA encoding vascular endothelial growth factor. *Ann Intern Med* 132: 880–884, 2000. doi:10.7326/0003-4819-132-11-200006060-00005.
3. **Brown RA, Phillips JB.** Cell responses to biomimetic protein scaffolds used in tissue repair and engineering. *Int Rev Cytol* 262: 75–150, 2007. doi:10.1016/S0074-7696(07)62002-6.
4. **Crafts TD, Jensen AR, Blocher-Smith EC, Markel TA.** Vascular endothelial growth factor: therapeutic possibilities and challenges for the treatment of ischemia. *Cytokine* 71: 385–393, 2015. doi:10.1016/j.cyto.2014.08.005.
5. **Eppler SM, Combs DL, Henry TD, Lopez JJ, Ellis SG, Yi JH, Annex BH, McCluskey ER, Zioncheck TF.** A target-mediated model to describe the pharmacokinetics and hemodynamic effects of recombinant human vascular endothelial growth factor in humans. *Clin Pharmacol Ther* 72: 20–32, 2002. doi:10.1067/mcp.2002.126179.
6. **Eremina V, Sood M, Haigh J, Nagy A, Lajoie G, Ferrara N, Gerber HP, Kikkawa Y, Miner JH, Quaggin SE.** Glomerular-specific alterations of VEGF-A expression lead to distinct congenital and acquired renal diseases. *J Clin Invest* 111: 707–716, 2003. doi:10.1172/JCI17423.
7. **Freedman SB, Isner JM.** Therapeutic angiogenesis for coronary artery disease. *Ann Intern Med* 136: 54–71, 2002. doi:10.7326/0003-4819-136-1-200201010-00011.
8. **Gasparini G.** Prognostic value of vascular endothelial growth factor in breast cancer. *Oncologist* 5, *Suppl* 1: 37–44, 2000. doi:10.1634/theoncologist.5-suppl_1-37.
9. **Groppa E, Brkic S, Bovo E, Reginato S, Sacchi V, Di Maggio N, Muraro MG, Calabrese D, Heberer M, Gianni-Barrera R, Banfi A.** VEGF dose regulates vascular stabilization through semaphorin3A and the neuropilin-1+ monocyte/TGF-β1 paracrine axis. *EMBO Mol Med* 7: 1366–1384, 2015. doi:10.15252/emmm.201405003.
10. **Henry TD, Annex BH, McKendall GR, Azrin MA, Lopez JJ, Giordano FJ, Shah PK, Willerson JT, Benza RL, Berman DS, Gibson CM, Bajamonde A, Rundle AC, Fine J, McCluskey ER, Investigators V; VIVA Investigators.** The VIVA trial: vascular endothelial growth factor in Ischemia for Vascular Angiogenesis. *Circulation* 107: 1359–1365, 2003. doi:10.1161/01.CIR.0000061911.47710.8A.
11. **Ho YT, Poinard B, Kah JC.** Nanoparticle drug delivery systems and their use in cardiac tissue therapy. *Nanomedicine (Lond)* 11: 693–714, 2016. doi:10.2217/nnm.16.6.
12. **Kadota S, Pabon L, Reinecke H, Murry CE.** In vivo maturation of human induced pluripotent stem cell-derived cardiomyocytes in neonatal and adult rat hearts. *Stem Cell Reports* 8: 278–289, 2017. doi:10.1016/j.stemcr.2016.10.009.
13. **Lee RJ, Springer ML, Blanco-Bose WE, Shaw R, Ursell PC, Blau HM.** VEGF gene delivery to myocardium: deleterious effects of unregulated expression. *Circulation* 102: 898–901, 2000. doi:10.1161/01.CIR.102.8.898.
14. **Maharaj AS, D'Amore PA.** Roles for VEGF in the adult. *Microvasc Res* 74: 100–113, 2007. doi:10.1016/j.mvr.2007.03.004.
15. **Miquerol L, Gertsenstein M, Harpal K, Rossant J, Nagy A.** Multiple developmental roles of VEGF suggested by a LacZ-tagged allele. *Dev Biol* 212: 307–322, 1999. doi:10.1006/dbio.1999.9355.
16. **Rodness J, Mihic A, Miyagi Y, Wu J, Weisel RD, Li RK.** VEGF-loaded microsphere patch for local protein delivery to the ischemic heart. *Acta Biomater* 45: 169–181, 2016. doi:10.1016/j.actbio.2016.09.009.
17. **Simón-Yarza T, Tamayo E, Benavides C, Lana H, Formiga FR, Grama CN, Ortiz-de-Solorzano C, Kumar MN, Prosper F, Blanco-Prieto MJ.** Functional benefits of PLGA particulates carrying VEGF and CoQ10 in an animal of myocardial ischemia. *Int J Pharm* 454: 784–790, 2013. doi:10.1016/j.ijpharm.2013.04.015.
18. **Street J, Bao M, deGuzman L, Bunting S, Peale FV Jr, Ferrara N, Steinmetz H, Hoeffel J, Cleland JL, Daugherty A, van Bruggen N, Redmond HP, Carano RA, Filvaroff EH.** Vascular endothelial growth factor stimulates bone repair by promoting angiogenesis and bone turnover. *Proc Natl Acad Sci USA* 99: 9656–9661, 2002. doi:10.1073/pnas.152324099.
19. **Takeshita S, Pu LQ, Stein LA, Sniderman AD, Bunting S, Ferrara N, Isner JM, Symes JF.** Intramuscular administration of vascular endothelial growth factor induces dose-dependent collateral artery augmentation in a rabbit model of chronic limb ischemia. *Circulation* 90: II228–II234, 1994.
20. **Xiong Q, Ye L, Zhang P, Lepley M, Swingen C, Zhang L, Kaufman DS, Zhang J.** Bioenergetic and functional consequences of cellular therapy: activation of endogenous cardiovascular progenitor cells. *Circ Res* 111: 455–468, 2012. doi:10.1161/CIRCRESAHA.112.269894.
21. **Ye L, Chang YH, Xiong Q, Zhang P, Zhang L, Somasundaram P, Lepley M, Swingen C, Su L, Wendel JS, Guo J, Jang A, Rosenbush D, Greder L, Dutton JR, Zhang J, Kamp TJ, Kaufman DS, Ge Y, Zhang J.** Cardiac repair in a porcine model of acute myocardial infarction with human induced pluripotent stem cell-derived cardiovascular cells. *Cell Stem Cell* 15: 750–761, 2014. doi:10.1016/j.stem.2014.11.009.
22. **Zaruba MM, Zhu W, Soonpaa MH, Reuter S, Franz WM, Field LJ.** Granulocyte colony-stimulating factor treatment plus dipeptidylpeptidase-IV inhibition augments myocardial regeneration in mice expressing cyclin D2 in adult cardiomyocytes. *Eur Heart J* 33: 129–137, 2012. doi:10.1093/eurheartj/ehr302.
23. **Zhu W, Shou W, Payne RM, Caldwell R, Field LJ.** A mouse model for juvenile doxorubicin-induced cardiac dysfunction. *Pediatr Res* 64: 488–494, 2008. doi:10.1203/PDR.0b013e318184d732.
24. **Zhu W, Soonpaa MH, Chen H, Shen W, Payne RM, Liechty EA, Caldwell RL, Shou W, Field LJ.** Acute doxorubicin cardiotoxicity is associated with p53-induced inhibition of the mammalian target of rapamycin pathway. *Circulation* 119: 99–106, 2009. doi:10.1161/CIRCULATIONAHA.108.799700.
25. **Zietz C, Rössle M, Haas C, Sendelhofert A, Hirschmann A, Stürzl M, Löhrs U.** MDM-2 oncoprotein overexpression, p53 gene mutation, and VEGF up-regulation in angiosarcomas. *Am J Pathol* 153: 1425–1433, 1998. doi:10.1016/S0002-9440(10)65729-X.